ON WAKE VORTEX RESPONSE FOR SEVERAL COMBINATIONS OF LEADING AND FOLLOWING AIRCRAFT

L.M.B.C.Campos, J.M.G.Marques
Instituto Superior Técnico
Av. Rovisco Pais 1049-001 Lisboa, Portugal

Abstract

The response of a following airplane to a pair of wing tip vortices left by a leading aircraft, represented by the Hallock-Burnham model, with added vorticity decay between the two aircraft. The effect of vorticity is evaluated as concerns the induced rolling moment and also the lift loss; these specify respectively the roll acceleration and the downward acceleration. The corresponding two response equations can be put into de same dimensionless form, and integrated using exponential integrals. This specifies the roll rate and sink rate as a function of time; besides the latter, the bank angle and altitude loss, are also plotted, all also as a function of time, for all combinations of leading and following aircraft in five classes. These are the three ICAO weight categories of light, medium and heavy, plus two other cases, viz. the special case of Boeing 757, which requires larger separations distances, and the case of very large aircraft, like the Very Large Transport Aircraft (VLTA).

1 Introduction

The effects of the wake of a leading aircraft on a following aircraft are one of the main factors determining separation distances on landing and take-off. Thus wake effects have implications both on: (i) airplane safety as concerns ability to retain roll control and contain height loss; (ii) runway capacity determined by aircraft spacing, which then impacts airport capacity and air traffic capacity. In addition, wake effects relate to aircraft design, in the sense that it is desirable to: (iii) reduce the strength of the wake of the leading aircraft; (iv) reduce the susceptibility of the following aircraft to wake effects. Thus the subject of wake effects relates both to aircraft design and air traffic management, justifying the existence of a vast literature on the subject (more than 1800 references to “wake”, “vortex” and “wake vortex”).

The specification of wake effects can lead to: (a) either the determination of a Safe Separation Distance (SSD), beyond which the following aircraft has enough roll control authority to cope with the wake of the leading aircraft; (b) the calculation of the response of the following aircraft to the wake of the leading aircraft at any distance. The knowledge of aerodynamics and flight dynamics required [1] is comparable in the two cases, the main difference being that the vorticity should be expressed as a function of distance to calculate the SSD in case (a), and as a function of time to calculate response in case (b). The response to wake effects may include, in addition to the roll effect, also an altitude loss; the two effects can combine to present a safety hazard, e.g. if a wake is encountered close to the ground in a landing approach.

Most of the vast literature on wake effects, of which a few examples are given [2-6], estimates wake effects using numerical methods. Analytical models have been developed assuming constant vortex strength [7]. The present model takes into account vortex decay in the analytical calculation of airplane response to a wake, as follows: (i) the lift loss (§2) and rolling moment (§3) due two wing tip vortices with axis parallel to the following aircraft are calculated; (ii) both involve the vorticity, whose decay with time is specified (§4) by dissipation by viscosity and convection

in the downwash of the leading aircraft; (iii) this specifies the rolling moment and lift loss of the following aircraft as a function of time, and thus the response (§5) in terms of respectively of roll and downward acceleration; (iv) the integration in dimensionless form leads to an exponential integral [8] in both cases, which specifies (§6) the roll rate and sink speed; (v) besides these, the bank angle and altitude loss, are also plotted as a function of time, for all (§7) combinations of leading and following aircraft in five categories: light, medium, special, heavy and very large. The discussion (§8) addresses the strengths of the present model, and its limitations to be considered in future work.

2 Effect of wake on lift loss

There several vortex models, e.g. those of Rankine [9], Lamb-Oseen [10], Hoffman-Joubert [11], Hallock-Burnham [12] and Proctor [13]. The difference between different vortex models is probably no greater then other uncertainties in the calculation of aircraft response to wake vortices. Thus the choice of a vortex model may not be critical, and the Hallock-Burnham (HB) model is chosen here because it has three desirable features: (i) it fits well with experimental data; (ii) it is specified by a single analytical expression valid for all radial distances from the "core" to the "external flow"; (iii) the analytical expression is of simple algebraic form, amenable to straightforward integration, to calculate induced lift loss and rolling moment. The tangential velocity of the HB-vortex is given as a function of radial distance r as by:

$$w(r) = \frac{\Gamma_0}{2\pi} \frac{r}{r^2 + a^2} . \qquad (1)$$

The tangential velocity is zero at the center $w(0) = 0$, grows linearly for small distance compared with the vortex core radius $w(r) \sim \Gamma_0 r / (2\pi a^2)$ for $r^2 << a^2$, and matches smoothly to a potential flow decay at large distances $w(r) \sim \Gamma_0 / (2\pi r)$ for $r^2 >> a^2$, going through a maximum at the vortex core radius:

$$w_{\max} \equiv w(a) = \Gamma_0 / 4\pi a = \Omega a , \qquad (2)$$

this value being used to specify the reference vorticity Ω, and to relate it to wake vortex strength:

$$\Gamma_0 = 4\pi a^2 \Omega . \qquad (3)$$

The vorticity will be reconsidered in §4. Thus the HB-vortex model is specified by:

$$w(r) = \frac{2\Omega a^2 r}{r^2 + a^2} , \qquad (4)$$

for a single vortex with axis at the origin.

The lift per unit span [14] is given by:

$$l(y) = \frac{1}{2} \rho C_L(\alpha) U^2 c(y) , \qquad (5)$$

where below the stall the lift coefficient is a linear function of angle of attack:

$$C_L(\alpha) = C_{L_\alpha} (\alpha - \bar{\alpha}) ; \qquad (6a)$$

the lift slope C_{L_α} is 2π for the Joukowsky airfoil [15] and takes values of that order of magnitude for other airfoils [16]. The lift is taken to be zero when aligned with the incident stream:

$$\bar{\alpha} = \frac{w(y)}{U} . \qquad (6b)$$

The substitution of (6b) into (6a) specifies (5) :

$$l(y) = \frac{1}{2} C_{L_\alpha} \rho c(y) U [U\alpha - w(y)], \qquad (7)$$

the lift per unit span. The lift loss per unit span due to the wake of leading aircraft impinging on the following aircraft is given by the second term on the r.h.s. of (7):

$$\Delta l(y) = -\frac{1}{2} C_{L_\alpha} \rho U c(y) w(y) \qquad (8)$$

and thus

$$\Delta L = -\frac{1}{2} C_{L_\alpha} \rho U \int_{-b/2}^{b/2} c(y)\, w(y)\, dy , \qquad (9)$$

specifies the total lift loss due to the vortex encounter. In this formula the lift coefficient was assumed to be a linear function of angle-of-attack (6a); in the applications that follow, the vortex encounter causes a lift loss, and thus a reduction of angle-of-attack. Thus, the airplane moves away from stall; the assumption of linear lift coefficient should hold for the initial disturbed motion.

3 Rolling moment induced by wake

Another effect of the vortex encounter is the rolling moment induced on the following aircraft by the wake of the leading aircraft:

$$R = \int_{-b/2}^{b/2} y\, \Delta l(y)\, dy\,, \qquad (10)$$

which relates to the lift loss (8) per unit span:

$$R = -\frac{1}{2} C_{L_\alpha} \rho U \int_{-b/2}^{b/2} y\, w(y) c(y)\, dy\,. \qquad (11)$$

Using the chord distribution for a trapezoidal wing and downwash for two dissimilar HB-vortices, the integrals:

$$\begin{aligned}\Delta L = &-\frac{2C_{L_\alpha}\rho U\bar{c}\Omega_r a_r^2}{1+\lambda}\times\\ &\times\int_{-b/2}^{b/2}\left(1+\frac{\lambda-1}{b}2|y|\right)\frac{y-y_r}{a_r^2+(y-y_r)^2}dy+\\ &+\frac{2C_{L_\alpha}\rho U\bar{c}\Omega_l a_l^2}{1+\lambda}\times\\ &\times\int_{-b/2}^{b/2}\left(1+\frac{\lambda-1}{b}2|y|\right)\frac{y-y_l}{a_l^2+(y-y_l)^2}dy\end{aligned}\,, \qquad (12)$$

$$\begin{aligned}R = &-\frac{2C_{L_\alpha}\rho U\bar{c}\Omega_r a_r^2}{1+\lambda}\times\\ &\times\int_{-b/2}^{b/2}\left(1+\frac{\lambda-1}{b}2|y|\right)\frac{y-y_r}{a_r^2+(y-y_r)^2}ydy+\\ &+\frac{2C_{L_\alpha}\rho U\bar{c}\Omega_l a_l^2}{1+\lambda}\times\\ &\times\int_{-b/2}^{b/2}\left(1+\frac{\lambda-1}{b}2|y|\right)\frac{y-y_l}{a_l^2+(y-y_l)^2}ydy\end{aligned}\,, \qquad (13)$$

specify the lift loss (12) and the rolling moment (13). The integrals will be evaluated the change of variable:

$$u = (y-y_r)/a_r\,, \qquad (14)$$

for the right-hand vortex, and similarly for the left-hand vortex.

The lift loss as:

$$\Delta L = -C_{L_\alpha}\rho U\bar{c}\left(\Omega_r a_r^2 f_r - \Omega_\ell a_\ell^2 f_\ell\right)/(1+\lambda)\,, \qquad (15)$$

where the dimensionless factor:

$$f_r = f_{1r} + \frac{\lambda-1}{b}\left(2y_r f_{2r} + 4a_r f_{3r}\right), \qquad (16)$$

involves (17a,b,c), and thus depends on the encounter geometry:

$$\begin{aligned}f_{1r} &\equiv \log\left\{\left[(b/2-y_r)^2+a_r^2\right]/\left[(b/2+y_r)^2+a_r^2\right]\right\}\\ f_{2r} &\equiv \log\left\{\left[a_r^2+b^2/4+y_r^2\right]^2-b^2y_r^2\right]/\left(a_r^2+y_r^2\right)^2\right\}\\ f_{3r} &\equiv \arctan\left[(b/2+y_r)/a_r\right]\\ &\quad-\arctan\left[(b/2-y_r)/a_r\right]-2\arctan\left(y_r/a_r\right)\\ f_{4r} &\equiv \arctan\left[(b/2+y_r)/a_r\right]+\arctan\left[(b/2-y_r)/a_r\right]\end{aligned} \qquad (17a\text{-}d)$$

The same factors (17a-d) appear in the rolling moment, viz.:

$$R = -\frac{1}{1+\lambda}C_{L_\alpha}\rho US\left(\Omega_r a_r^2 h_r - \Omega_r a_l^2 h_l\right), \qquad (18)$$

where:

$$\begin{aligned}h_r &= 2+(y_r/b)f_{1r}-2(a_r/b)f_{4r}+(\lambda-1)\\ &\times\left\{1+2\left[\left(y_r^2-a_r^2\right)/b^2\right]f_{2r}+8\left(a_r y_r/b^2\right)f_{3r}\right\}.\end{aligned} \qquad (19)$$

4 Vorticity decay with time due to viscosity

The dependence of the rolling moment (18) and lift loss (15) on time is specified by the vorticities $\Omega_r(t)$ and $\Omega_l(t)$. Starting from the Navier-Stokes equation [18]

$$\begin{aligned}&\frac{\partial\vec{V}}{\partial t}+\nabla\left(V^2/2\right)+\left(\nabla\times\vec{V}\right)\times\vec{V}+\\ &+\rho^{-1}\nabla p=\eta\nabla^2\vec{V}+\left(\varsigma+\eta/3\right)\nabla\left(\nabla.\vec{V}\right)\end{aligned}\,, \qquad (20)$$

in the incompressible case, by taking the curl, leads to a convected diffusion equation,

$$\nabla.\vec{V}=0: \qquad \frac{\partial\vec{\Omega}}{\partial t}+\nabla\times\left(\vec{\Omega}\times\vec{V}\right)=\eta\nabla^2\vec{\Omega}\,, \qquad (21)$$

satisfied by the vorticity:

$$\vec{\Omega}\equiv\nabla\times\vec{V}\,. \qquad (22)$$

In the present case of mean flow velocity consisting of an uniform stream plus a downwash (23a)

$$\vec{V}=U\vec{e}_x+w\vec{e}_z\,, \quad \vec{\Omega}=\Omega\vec{e}_x \qquad (23a,b)$$

and vorticity is aligned with the aircraft axis (23b), and the second term of the vorticity equation (21) is:

$$\nabla\times\left(\vec{V}\times\vec{\Omega}\right)=\vec{e}_x\frac{\partial(w\Omega)}{\partial z}-\vec{e}_z\frac{\partial(w\Omega)}{\partial x}\,; \qquad (24)$$

if longitudinal derivatives are smaller than transverse ones, the first term in (24) predominates.

In the latter case the vorticity equation reduces to its x-component,viz.:

$$\frac{\partial \Omega}{\partial t}+\frac{\partial (w\Omega)}{\partial z}=\eta\left(\frac{\partial^2 \Omega}{\partial y^2}+\frac{\partial^2 \Omega}{\partial z^2}\right), \qquad (25)$$

This is a scalar heat equation [19], with convective term. A point vortex of circulation strength Γ_0 is taken as the source:

$$\frac{\partial \Omega}{\partial t}+\frac{\partial (w\Omega)}{\partial z}-\eta\left(\frac{\partial^2 \Omega}{\partial y^2}+\frac{\partial^2 \Omega}{\partial z^2}\right)=\Gamma_0 \delta(x)\delta(y), \qquad (26)$$

with δ denoting the Dirac delta function. The solution of (26) is [20]:

$$\Omega(t,y,z)=\frac{\Gamma_0}{2\pi\eta(t-z/w)}\exp\left(-\frac{y^2+z^2}{2\eta(t-z/w)}\right). \qquad (27)$$

The wake of the leading aircraft is thus represented at the following aircraft as due to a point vortex of circulation strength Γ_0, which is an approximate representation if the two aircraft are at a large distance compared to wing parameters. The transverse coordinates disappear from the vorticity (27) by identifying them with the vortex radius, $y^2+z^2=a^2$:

$$\Omega(t,z)=\frac{\Gamma_0}{2\pi\eta(t-z/w)}\exp\left(-\frac{a^2}{2\eta(t-z/w)}\right). \qquad (28)$$

The longitudinal coordinate may also be omitted if the separation between the aircraft is large enough, $t=x/U >> z/w$:

$$\Omega(t)=\frac{\Gamma_0}{2\pi\eta t}\exp\left(-\frac{a^2}{2\eta t}\right), \qquad (29)$$

leaving only the time dependence in the vorticity.

The vorticity (29) is proportional to the vortex circulation strength Γ_0 of the leading aircraft, which is calculated next. The lift per unit span is given by Joukowski theorem [14,15].

$$l(y)=\rho U\Gamma(y), \qquad (30)$$

so that comparison with (5) specifies the circulation

$$\Gamma(y)=\frac{1}{2}C_L(\alpha)Uc(y). \qquad (31)$$

For straight steady and level flight the weight equals the lift:

$$W=\frac{1}{2}\rho U^2 S C_L(\alpha), \qquad (32)$$

and hence the vortex strength is specified by the circulation at the wing root:

$$\Gamma_0\equiv\Gamma(0)=\frac{1}{2}C_L(\alpha)Uc_r=\frac{c_r W}{\rho U S}, \qquad (33)$$

in terms of aircraft parameters. Note that the vorticity (29) is zero at the trailing edge of the leading aircraft $\Omega(0)=0$ because the flow is potential, then increases with time as the vortex rolls up, reaching a maximum $\Omega_{\max}=\Gamma_0/(2\pi a^2\rho)$ at a time $t_*=a^2/2\eta$, after which the viscosity, besides limiting growth, causes ultimate decay $\Omega(\infty)=0$. Substitution of (33) in (29) specifies the vorticity laws:

$$\Omega(t)=\frac{c_{r_1}W_1}{2\pi\rho U_1 S_1 \eta t}\exp\left(-\frac{a^2}{2\eta t}\right), \qquad (34)$$

where the index "1" refers to the leading aircraft.

5 Airplane response to the wake encounter

The downward acceleration

$$m\ddot{z}=\Delta L, \qquad (35)$$

is associated with the lift loss (15). The vortex radii will be taken the same $a_l=a_r=a$, so that the vorticity decay law (34) is the same for the right and the left hand vortices:

$$a_l=a_r=a: \quad 2\Omega_{\pm}(t)\equiv\Omega_r(t)\pm\Omega_l(t), \qquad (47a,b)$$

and it will be shown in the sequel that: (i) the sum of vorticities is relevant to the lift loss; (ii) the difference of vorticities is relevant to the rolling moment. Using (47), the lift loss (15) is given by:

$$\Delta L=-\frac{2}{1+\lambda}C_{L_\alpha}\rho U\bar{c}a^2\Omega_+(t)f, \qquad (36)$$

where the average encounter factor f for the lift loss is defined by:

$$\Omega_r f_r-\Omega_l f_l\equiv f(\Omega_r+\Omega_l)=2f\Omega_+. \qquad (37)$$

This will be obviously met by symmetrical vortices, since $y_r=-y_l$ implies $f_r=-f_l\equiv f$ by (16; 17a-d) and then (37) reduces to (47a); for opposite right and left vorticites

$\Omega_r = \Omega_l = \Omega_0$, it follows that $\Omega_+ = 2\Omega_0$ by (47a) and hence by (36) there is a double lift loss. In general for unsymmetrical vortices $y_r \neq y_l$ and/or unequal vorticities $\Omega_r \neq \Omega_l$, and f satisfying (37) can be found using f_r in (16) and a similar expression for f_l. Substituting (36) in (35) the vertical acceleration in shown to be:

$$m_2 \ddot{z} = -\frac{2f}{1+\lambda} C_{L_\alpha} \rho U_2 S_2 \frac{a}{b_2} a \Omega_+(t), \qquad (38)$$

where the index "2" refers to the following aircraft.

The roll acceleration

$$I \ddot{\phi} = R, \qquad (39)$$

is due to the rolling moment (18) where as in (35) a linear uncoupled response is assumed, for the initial stages of the disturbance following the vortex encounter. This linear response applies at least up to a bank angle $\phi = 10^o$, which is the airline rule of a mandatory go-round in case of a wake vortex encounter on approach to land. For a short time, damping effects are also neglected. For identical vortex core radii, it is given by:

$$a_r = a_l \equiv a: \quad R = -\frac{C_{L_\alpha} \rho U S}{1+\lambda} a^2 h \Omega_-(t), \qquad (40)$$

where the average encounter factor for the rolling moment h is defined by:

$$\Omega_r h_r - \Omega_l h_l \equiv (\Omega_r - \Omega_l) h = 2h\Omega_-. \qquad (41)$$

In the case of symmetric vortices $y_r = -y_l$, since $h_r = h_l$ by (19) then (41) is an identity, taking into account (47b); in the particular case of symmetrical vortices $h_r = h_l$ and opposite vorticities $\Omega_r = \Omega_l$ then $\Omega_r h_r - \Omega_l h_l = 0$ there is no rolling moment; in the general case of unsymmetrical vortices $y_r \neq -y_l$ and of dissimilar vorticities $\Omega_r \neq \Omega_l$ the condition (41) specifies h, in terms of h_r (19) and h_l. Substitution of (41) in (39) yields:

$$I_2 \ddot{\phi} = -\frac{2 C_{L_\alpha} h}{1+\lambda} \rho U_2 S_2 a^2 \Omega(t). \qquad (42)$$

Using (34) for the vorticity dependence on time, for wing tip vortices with the same radius, leads to:

$$I_2 \ddot{\phi} = -\frac{2h}{1+\lambda} \frac{U_2}{U_1} \frac{S_2}{S_1} W_1 a \frac{c_{r_1} a}{\eta t} \exp\left(-\frac{a^2}{2\eta t}\right). \qquad (43)$$

6 Sink speed and roll rate

The exponentials suggest the introduction of a dimensionless time τ, which is the ratio of time t to the time $a^2/2\eta$ of peak vorticity of a vortex of core radius a due in the presence of the turbulent viscosity η in (44a):

$$\tau \equiv \frac{2\eta t}{a^2}; \qquad \frac{d^2 z}{d\tau^2} = \left(\frac{a^2}{2\eta}\right)^2 \ddot{z}, \qquad (44a,b)$$

using the dimensionless time in the downward acceleration (44b) leads to:

$$\frac{d^2 X}{d\tau^2} = \frac{A}{\tau} \exp\left(-\frac{1}{\tau}\right), \qquad (45)$$

with $X \equiv z/a$ and

$$A \equiv -\frac{f}{1+\lambda} \frac{C_{L_\alpha}}{2\pi} \frac{W_1}{W_2} \frac{S_2}{S_1} \frac{U_2}{U_1} \frac{a}{b_2} \frac{g c_{r_1} a^2}{\eta^2}. \qquad (46a,b)$$

The same transformations (44b) may be applied to (58) the roll acceleration, leads to the same dimensionless form (45) for the bank angle $X \equiv \phi$, which is dimensionless:

$$A \equiv -\frac{h}{1+\lambda} \frac{C_{L_\alpha}}{2\pi} \frac{W_1}{W_2} \frac{U_2}{U_1} \frac{S_2}{S_1} \left(\frac{a}{r_2}\right)^2 \frac{g c_{r_1} a^2}{\eta^2}. \qquad (47a,b)$$

The integration of the dimensionless response for the acceleration (45) specifies the dimensionless velocity change between dimensionless times τ_1 e τ_2:

$$\frac{dX}{d\tau} = A \int_{\tau_1}^{\tau_2} \frac{e^{-1/\tau}}{\tau} d\tau. \qquad (48)$$

A change of variable:

$$T \equiv 1/\tau: \qquad \frac{dX}{d\tau} = A \int_{T_2}^{T_1} \frac{e^{-T}}{T} dT, \qquad (49)$$

leads to [8] the exponential integral:

$$E(\xi) \equiv \int_{\xi}^{+\infty} \frac{e^{-T}}{T} dT, \qquad (50)$$

so that the dimensionless velocity is specified:

$$\frac{dX}{d\tau} = A\left[E\left(1/\tau_2\right) - E\left(1/\tau_1\right)\right], \qquad (51)$$

by the difference of two exponential integrals. If the starting time is taken to be that of the formation of the vortex at the trailing edge of the wing of the leading aircraft, then

$$\tau_1 = 0,\ T_1 = \infty,\ \ E\left(T_1\right) = 0\,, \qquad (52)$$

and only one exponential integral appears in the dimensionless velocity:

$$\tau_1 = 0,\ \tau_2 = \tau: \qquad \frac{dX}{d\tau} = AE\left(1/\tau\right)\,. \qquad (53)$$

The transformation from dimensionless time (44a) to time:

$$\frac{dX}{dt} = \frac{2\eta}{a^2}\frac{dX}{d\tau}\,, \qquad (54)$$

specifies the dimensional velocity from the dimensionless one. Substituting (44a,63) in (53) the rate equation is:

$$\frac{dX}{dt} = \frac{2\eta}{a^2} AE\left(\frac{a^2}{2\eta t}\right). \qquad (55)$$

7 Altitude loss and bank angle

It has been shown that the dimensionless altitude (46a) and the roll angle (47a) satisfy the same acceleration equation (45), in terms of the dimensionless time (44a), where the difference appears only in the constant A, which is specified by (46b) for the altitude and by (47b) for the roll angle. It follows that the dimensionless sink speed and roll rate satisfy the same equation (53), viz.:

$$\frac{d}{d\tau}\left(\frac{X}{A}\right) = E\left(\frac{1}{\tau}\right)\,. \qquad (56)$$

In order to apply the preceding results in numerical form, example aircraft are chosen, in each of the five categories indicated in *Table I*: (i) the light, medium and heavy categories correspond to the ICAO classification by maximum take-off weight, for the purpose of setting separation distances; (ii) the Boeing 757-200 has been added as a "special" aircraft class since it requires larger separation than other aircraft in this weight category, according to FAA rules; (iii) a VLTA has been added as a "very large" class, to represent future airliners significantly larger than the Boeing 747-400, to assess whether they would justify the creation of an additional ICAO or FAA category "super-heavy".

Table I– The five classes of aircraft, viz. the three ICAO categories plus special and very large, with their symbols, and the examples chosen for the response plots in figures 1 to 5.

Designation	Symbol	Example
ICAO: Light	ℓ	Citation 500
ICAO: Medium	m	B737-700
Special	s	B 757-200
ICAO: Heavy	h	B747-400
Very Large	v	VLTA

The data on each of the chosen aircraft in the five classes consisting of manufacturer data from open sources [21,22].

The two wing tip vortices were assumed to have equal core radii $a_r = a_l = a$, and the separation between the wing tip vortices of the leading aircraft to reduce to $b_1/\pi = 0.318\,b_1$; also, it is assumed (*Figure 2*) that the following aircraft flies parallel to the leading aircraft offset a distance $y_0 = -b_2/8 = -0.125\,b_2$ to the left.

The 25 combinations are illustrated in *Figures 1 to 5* respectively for light (ℓ), medium (m), special (s), heavy (h) and very large (v) aircraft leading; in each figure the five classes of following aircraft are considered, viz. v, h, s, m, l. Each figure consists of two panels, with altitude loss (top) and bank angle (bottom).

For a leading light aircraft (*Figure 1*), altitude loss is quite small, which is quite noticeable since the same scale $0 \le z \le 5m$ has been taken for the plots for all 25 encounters in Figures 1 to 5. Although the same scale has been taken also for bank angle $|\phi| \le 30^\circ$, the roll response to a light leading aircraft is visible, and more pronounced for a light following aircraft.

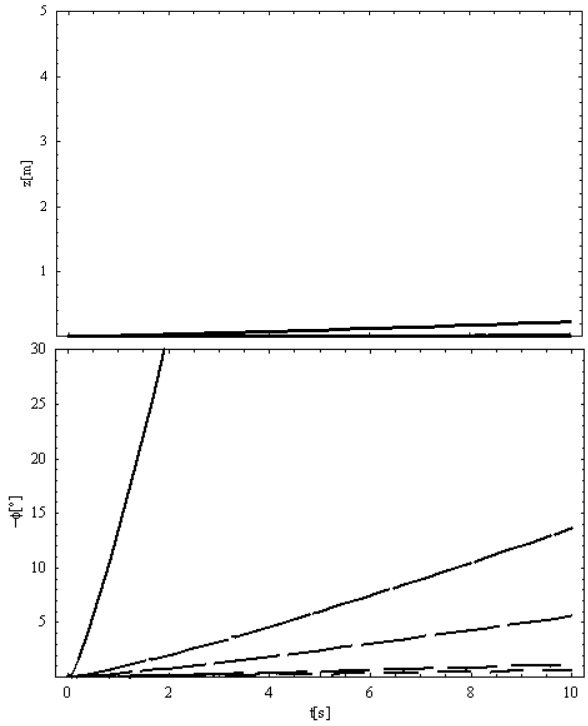

Figure 1 Altitude loss (top) and bank angle (bottom), as function of time *versus* time for light leading aircraft, followed by very large, heavy, special, medium and light aircraft.

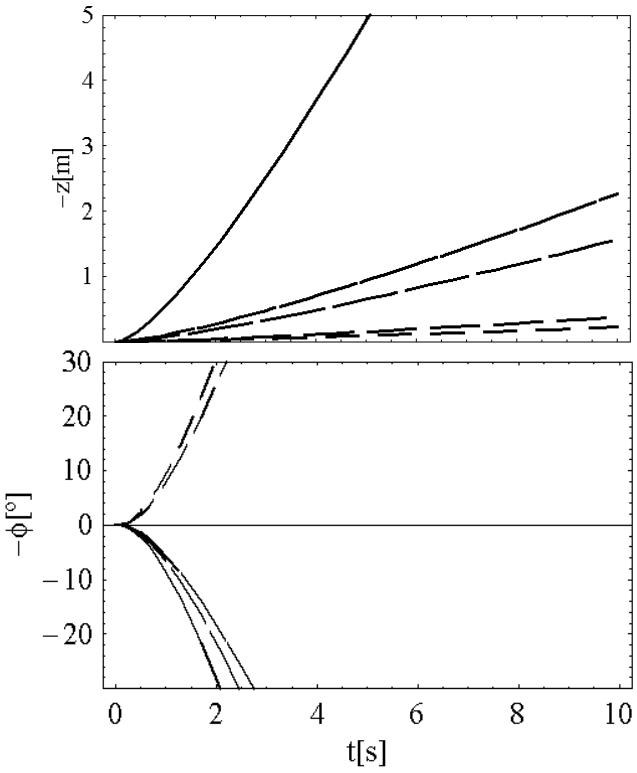

Figure 3 As figure 1 for special leading aircraft.

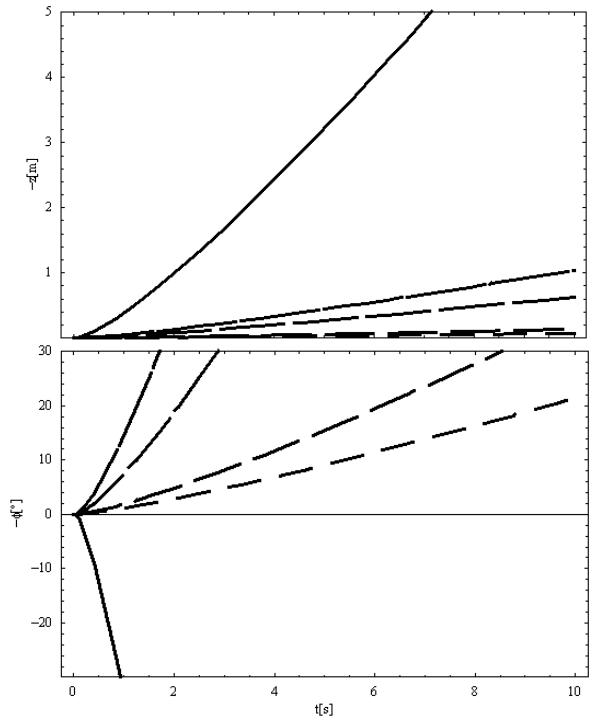

Figure 2 As figure 1 for medium leading aircraft.

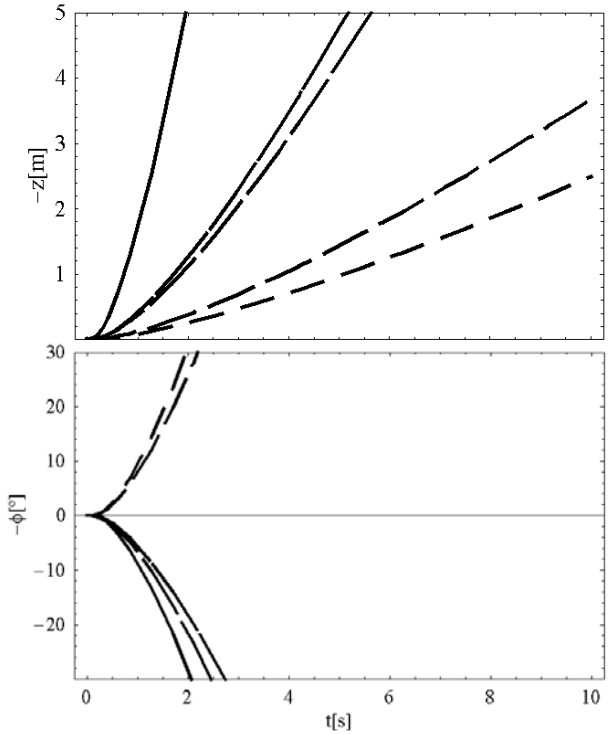

Figure 4 As figure 1 for heavy leading aircraft.

If a medium aircraft is leading (*Figure 2*) the altitude loss (top) are noticeable for a light following aircraft, and bank angle (bottom) show significant response, except for the heavy and large aircraft. A light aircraft following a medium aircraft rolls in opposite direction to allother four classes of following aircraft, because it catches only one vortex from the leading aircraft, viz. that coming from the right wing tip. The case of special leading aircraft (*Figure 3*) shows smaller response for the heavy and large following aircraft, and increasing response for the special, medium and light aircraft, with the light aircraft rolling in opposite directions to all others, for the same reason of catching only one wing tip vortex from the leading aircraft. The case of heavy leading aircraft (*Figure 4*) causes significant response in all following aircraft except the large, and now the light and medium following aircraft roll in opposite direction to the other three classes. The large leading aircraft (*Figure 5)* causes the largest response in the following aircraft, with the light, medium and special rolling in opposite direction to the heavy and large following aircraft.

The times to ten-degree bank angle listed in Table II can be read-off the bottom panel of Figures 1 to 5, which indicate bank angle response.

Table II Time in seconds to reach a bank angle $\phi = 10^{o}$ which is the airline limit for mandatory go-round (leading in columns).

	ℓ	**m**	**s**	**h**	**v**
ℓ	0.798	0.438	0.544	0.818	1.090
m	7.683	0.770	0.847	1.028	1.398
s	16.50	1.253	0.945	3.807	1.270
h	66.38	3.537	2.284	1.013	1.147
v	114.3	5.393	3.232	1.153	1.040

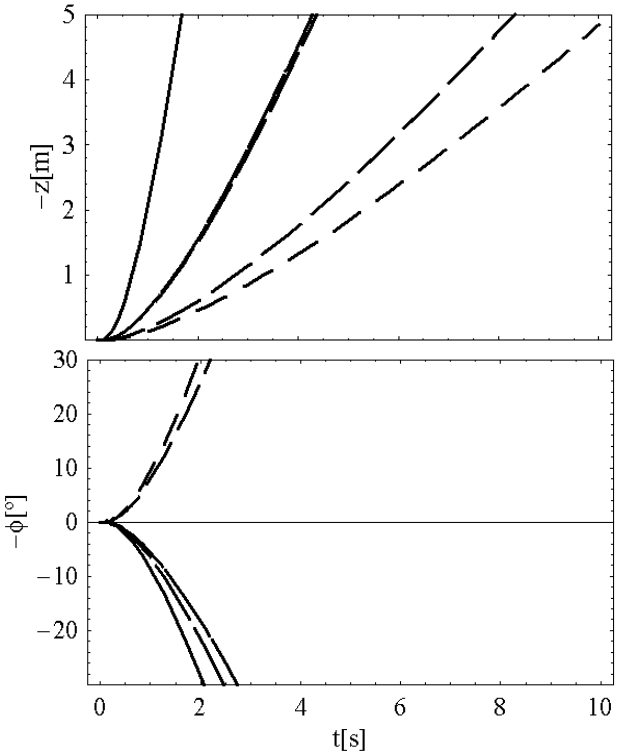

Figure 5 As figure 1 for very large leading aircraft.

A bank angle of ten degrees is reached quickly, for a light leading aircraft, only if the following aircraft is also light; as the leading aircraft moves up the scale, to medium, special, heavy and large, so the times to ten-degree bank angle become short for more classes of following aircraft. In the case of heavy or large leading aircraft, the times to ten-degree bank angle are short and of the order of one second for all classes of following aircraft. The exception of slower response for a special aircraft following a heavy, is a special case of a following aircraft on the "borderline" between those rolling to the right and those rolling to the left; this means that the wing tip vortices from the leading aircraft hit the following aircraft at an asymmetric position which happens to produce a smaller rolling moment. The opposite case, of very quick roll is that of a smaller following aircraft catching only one wing tip vortex from a bigger leading aircraft.

The conclusions both from Figures 1 to 5 and Table II are: (i) the roll response is more significant for bigger leading aircraft (in the scale light, medium, special, heavy and large),

and smaller following aircraft; (ii) the roll response may be reduced in cases where the two wing tip vortices almost counter each other, but this a fortuitous case which cannot be relied upon; (iii) an unfortunate situation which is certain to increase roll response, is when a smaller following aircraft catches only one wing tip vortex from a bigger leading aircraft. The Figures 1 to 5 represent an upper bound or a worst case scenario in which the following aircraft will hit the whole vortex from the time of generation, viz. they concern the response of the following aircraft in the conditions (53), i.e. assuming it experiences the entire time evolution of the wake of the leading aircraft, from the initial potential flow, to the vortex roll-up and subsequently decay due to viscosity; if only a part of the vortex wake evolution is considered, then (51) must be used, subtracting the term $E(T_1)$ due to the evolution before the time $\tau_1 = 1/T_1$.

In Figure 6 the case of heavy leading aircraft and medium following aircraft is considered with vortex starting times $t_0/t_* = 0,1,2,5,10$ a multiple of the peak vorticity time. It is seen in *Figure 6* that if the following aircraft encounters the wake vortex of the leading aircraft with greater separation, the induced sink rate (top left) is initially smaller, and thus takes longer (bottom left) to build-up to the same altitude loss; a similar remark can be made with regard to roll rate (top right), which is initially smaller for larger separation distance, although the bank angle (bottom right) still builds-up quite fast.

The vortex wake of the leading aircraft was considered to be the only effect on vertical acceleration (35) and roll acceleration (39) of the following aircraft, thus isolating this aspect, to illustrate better its consequences. It is clear that these results could be extended by including the damping terms, which become important for longer times, in limiting rates e.g. roll or sink rates.

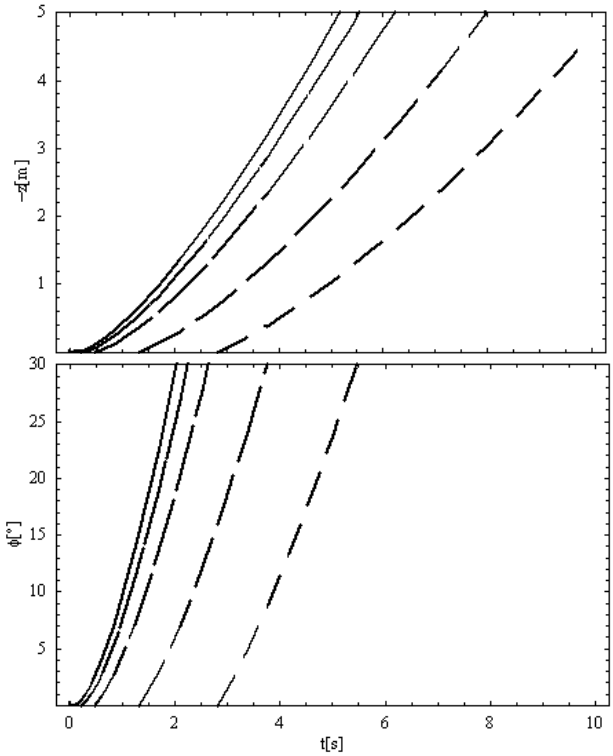

Figure 6 As figure 1 for heavy leading aircraft and ligth following aircraft, with starting time at a multiple of the peak vorticity time $t_0/t_* = 0,1,2,5,10$.

Also, the effect of control surface deflections are important in limiting flight deviations, e.g. roll angles and altitude loss. The coupling of vertical acceleration to pitch and longitudinal motions, and the coupling of roll to yaw and sideslip are generally less important [7] than the effects of control surfaces and damping.

The encounter geometry considered was very simple, in that the following aircraft flies parallel to the wake of the leading aircraft, staying indefinitely at a constant lateral distance from the axis. In a vortex crossing configuration, the wake effects are more transient, and can lead not to a roll to one side only, but rather to a large wing rock motion. The effect of distinct vortex "core" and "external flow" models on the wake vortex encounter has been another subject of investigation.

References

[1] Campos, L.M.B.C., Marques, J.M.G., 2002 "On the calculation of safe separation distances between aircraft due to turbulent wakes" (in preparation)

[2] Shen, S, Ding, F, Han, J., Lin, Y-L., Arya, S. P. & Proctor, F. H. 1999 "Numerical modeling studies of wake vortices: real case simulations", AIAA Paper 99-0755, 37th Aerospace Sciences Meeting, Reno, Nevada.

[3] Vicroy, D. D. & Nguyen, T. 1993 "A numerical simulation study to develop an acceptable wake encounter boundary for a B737-100 airplane", AIAA paper.

[4] Perry, R. R., Hinton, D. A. & Stuever, R. A. 1996 "NASA wake vortex research for aircraft spacing" AIAA paper.

[5] Hinton, D.A. 1996 "An Aircraft Vortex Spacing System (AVOSS) for dynamical wake vortex spacing criteria", 78th Fluid Mechanics Panel & Symposium on the Characterization and modification of wakes from lifting vehicles in fluids, Trondheim, Norway.

[6] Hinton, D.A., Charnock, J.K., Bagwell, D.R. & Grigsby, D. 1999 "NASA Aircraft Vortex Spacing System Development Status", AIAA 37thAerospace Sciences Meeting, Reno, Nevada.

[7] Jackson, W. (ed) 2001 "Wake Vortex Prediction: An Overview, Appendix F: Hazard Definition", Transportation Department of Canada TP 13629E.

[8] Abramowitz, M., Stegun, I. 1965 *Tables of mathematical functions*. Dever.

[9] Hinton, D.A. & Tatnall, C.R. 1997 "A candidate wake vortex strength definition for application to the NASA Aircraft Vortex Space System (AVOSS)" NASA Tech. Memo TM-110343.

[10] Lamb, H. 1932 *Hydrodynamics*. Cambridge U.P., 6th ed.

[11] Hoffman, E.R. & Joubert, P.N. 1963 Turbulent Line Vortices. *J. Fluid Mech.* **16**, 395-411.

[12] Hallock, J.N. & Burnham, D.C. 1997 Decay characteristics of wake vortex from jet transport aircraft AIAA paper 97-0060, 35th Aerosp. Sci. Meet. Exhib. 9-10 Jan., Reno, NV.

[13] Proctor, F. H. 1998 The NASA-Langley wake vortex modeling effort in support of an operational aircraft spacing system. AIAA paper 98-0589.

[14] Lighthill, M.J. 1986 *An informal introduction to fluid mechanics*, Oxford U.P.

[15] Milne-Thomson, L.M. 1958 *Theoretical Aerodynamics.* Dover, New York.

[16] Abott,I.H. & Doenhoff, A.E. 1959 *Theory of wing sections.* Dover.

[17] Tatnall, C.R. 1995 "A proposed methodology for determining wake-vortex imposed aircraft separation constraints", M. Sc. thesis submitted at George Washington University.

[18] Batchelor, G.K. 1967 *Fluid Mechanics*. Cambridge U.P.

[19] Carslaw, H.S. & Jaeger, J.C. 1949 *Heat conduction in solids*, Oxford U.P.

[20] Landau, L.D. & Lifshitz, E.F. 1953 *Fluid Mechanics*. Pergamon, Oxford.

[21] Jackson, P. 2000 *Jane's All-the-World's Aircraft* 2000-2001. MacDonald and Jane's, London.

[22] Stuerver, R.A. Airplane data base for wake-vortex hazard definition and assessment, version 2.0, NASA Langley Research Center.